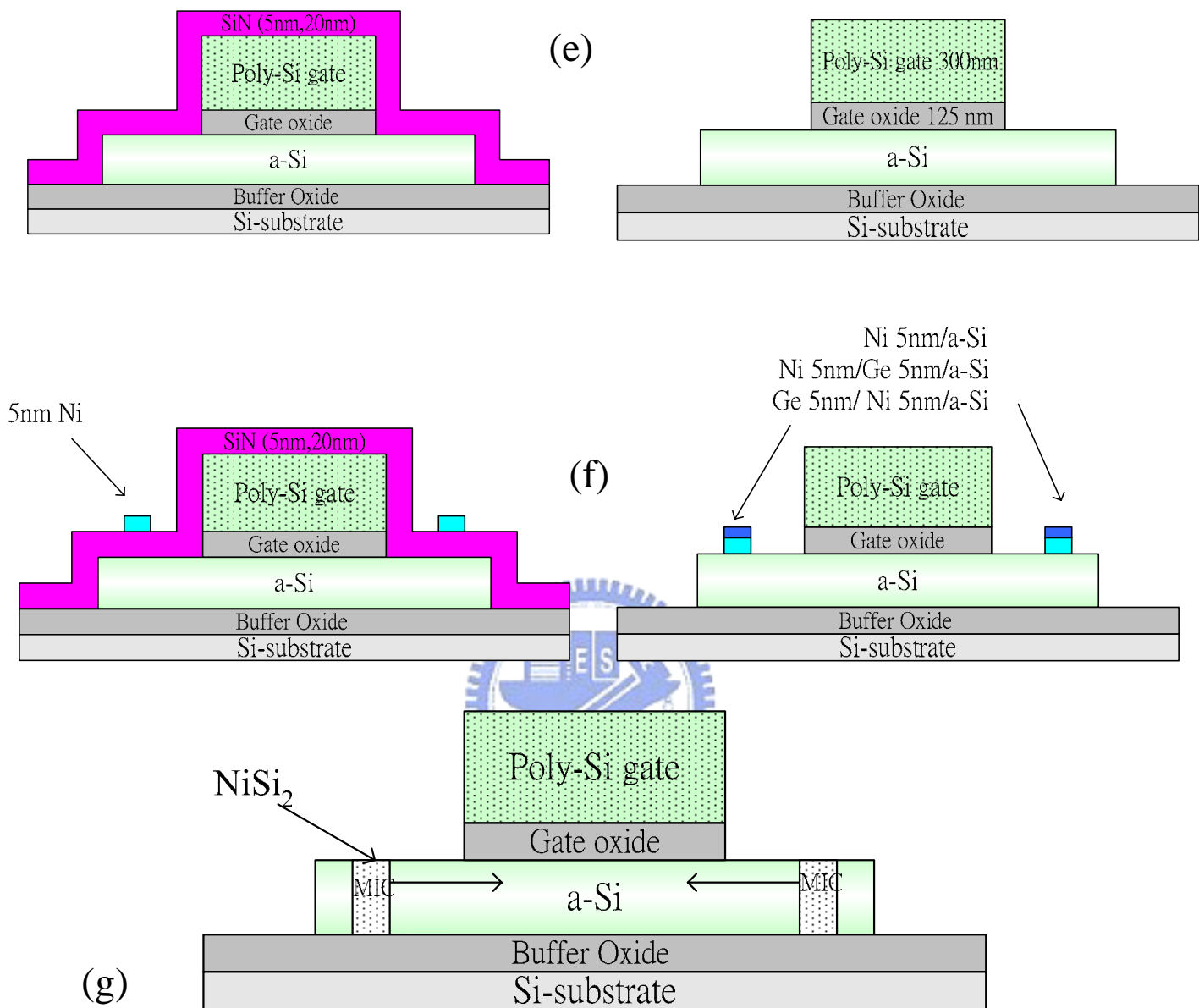
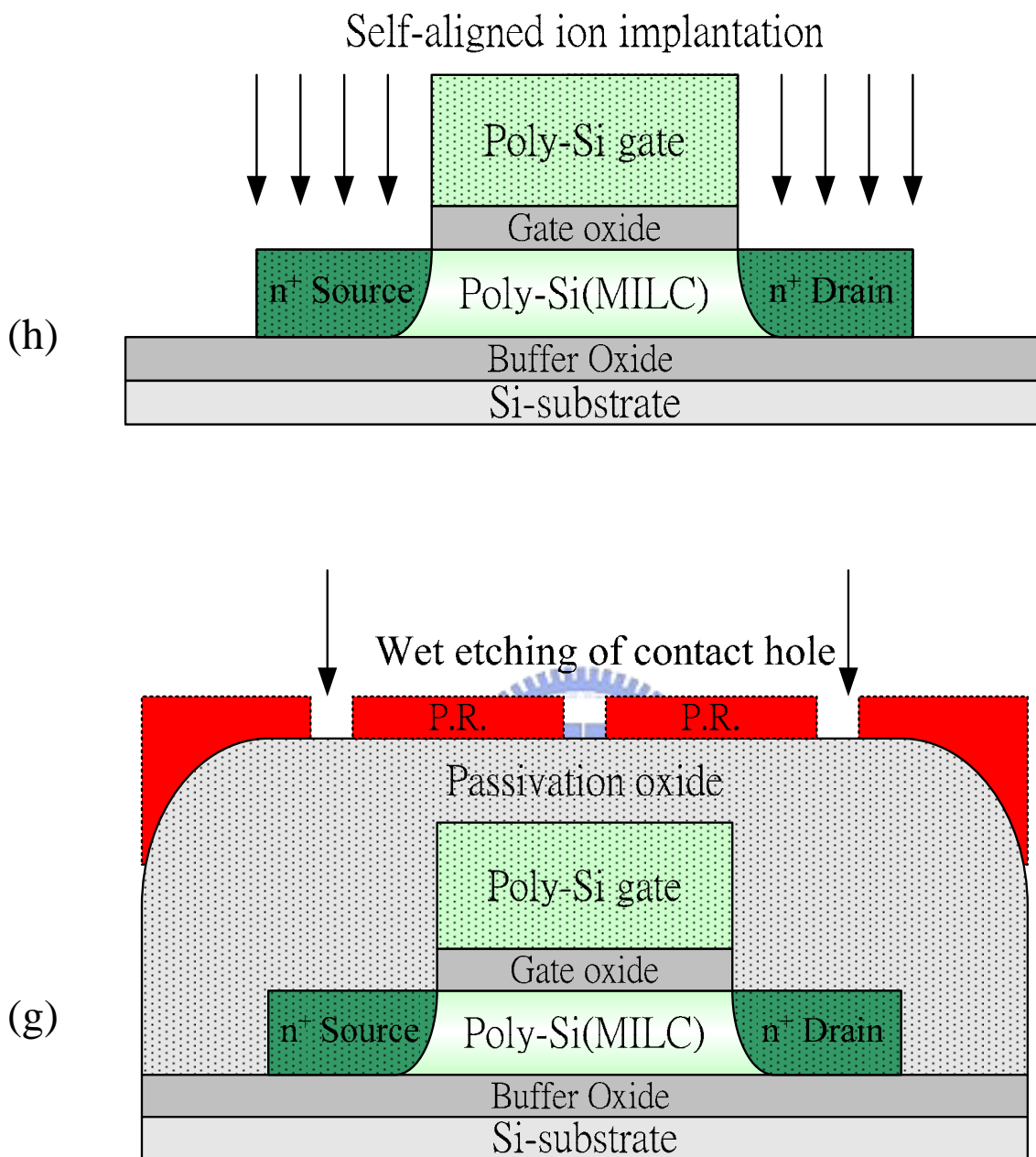


**Figure 3-1** Process flow of MILC n-channel TFT's with Ge Layer and Si<sub>3</sub>N<sub>4</sub> NanoCap Layer.



**Figure 3-1** Process flow of MILC n-channel TFT's with Ge Layer and Si<sub>3</sub>N<sub>4</sub> NanoCap Layer.



**Figure 3-1** Process flow of MILC n-channel TFT's with Ge Layer and  $\text{Si}_3\text{N}_4$  NanoCap Layer.

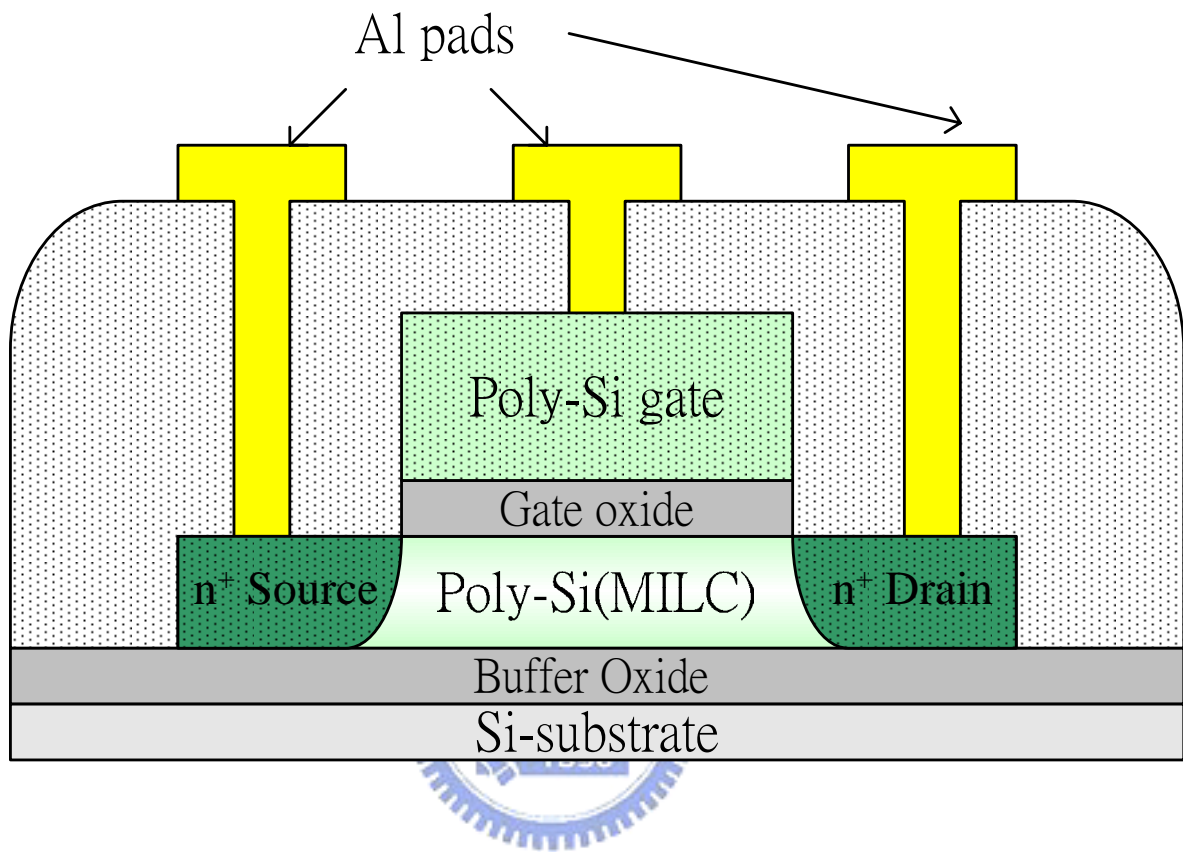


**Figure 3-1** Process flow of MILC n-channel TFT's with Ge Layer and  $\text{Si}_3\text{N}_4$  NanoCap Layer.

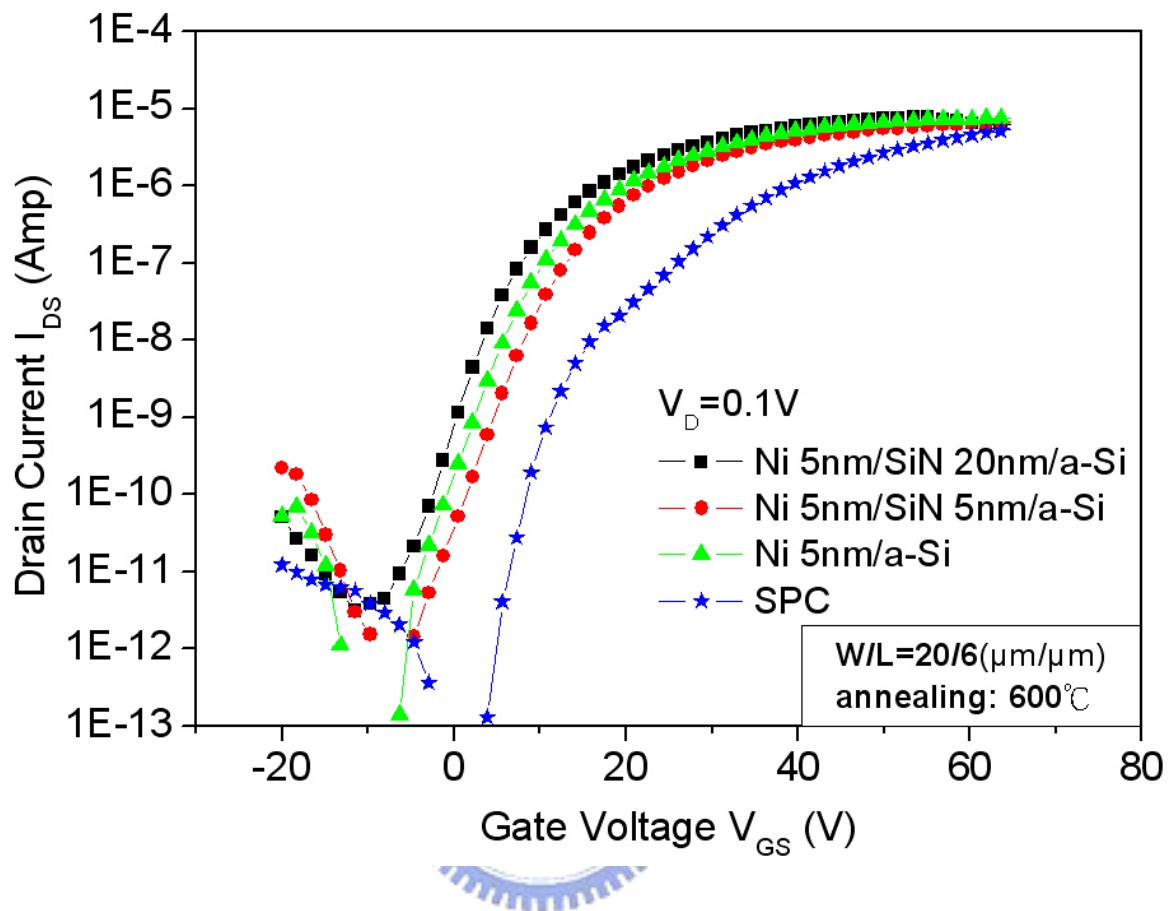


Figure 3.2 Transfer characteristics for comparison of MILC TFT's with and without  $\text{Si}_3\text{N}_4$  filter layer ( $V_D=0.1V$ ).

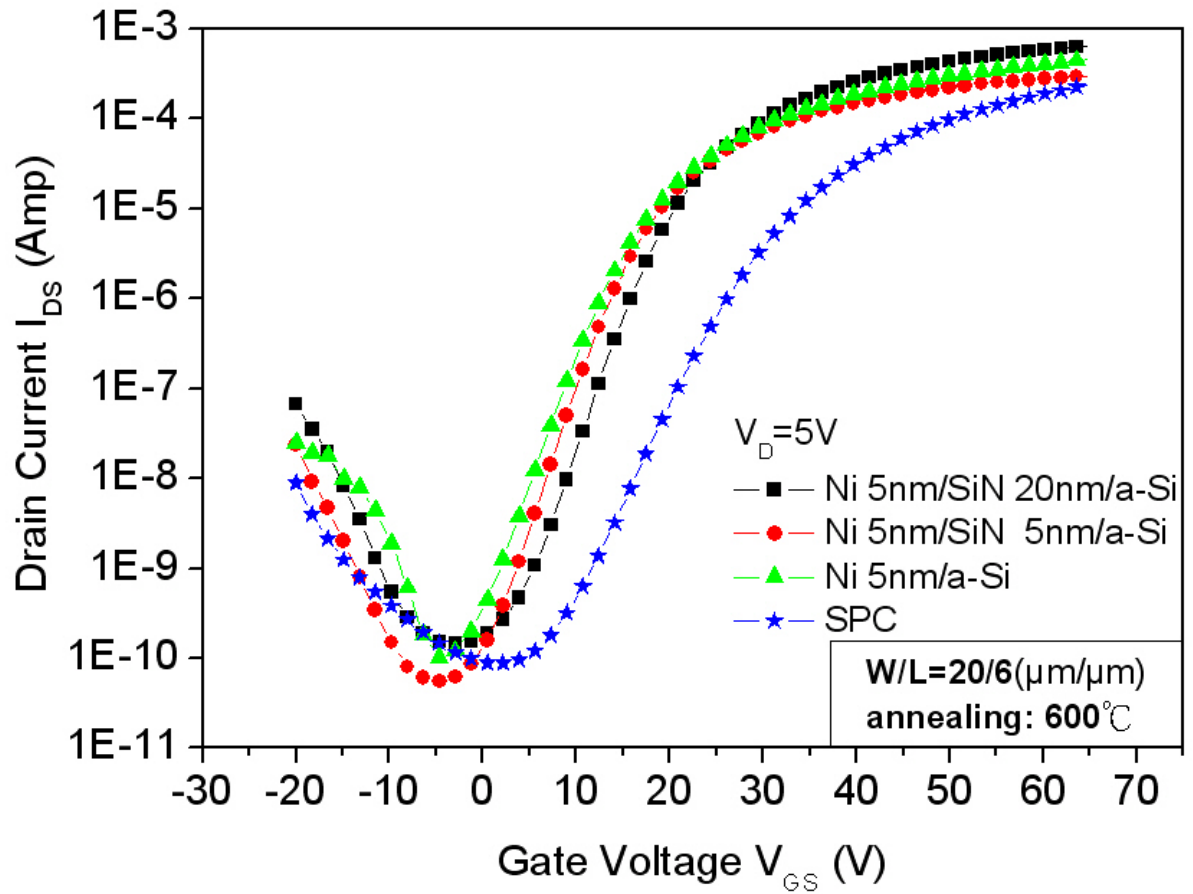


Figure 3.3 Transfer characteristics for comparison of MILC TFT's with and without  $Si_3N_4$  filter layer ( $V_D=5V$ ).

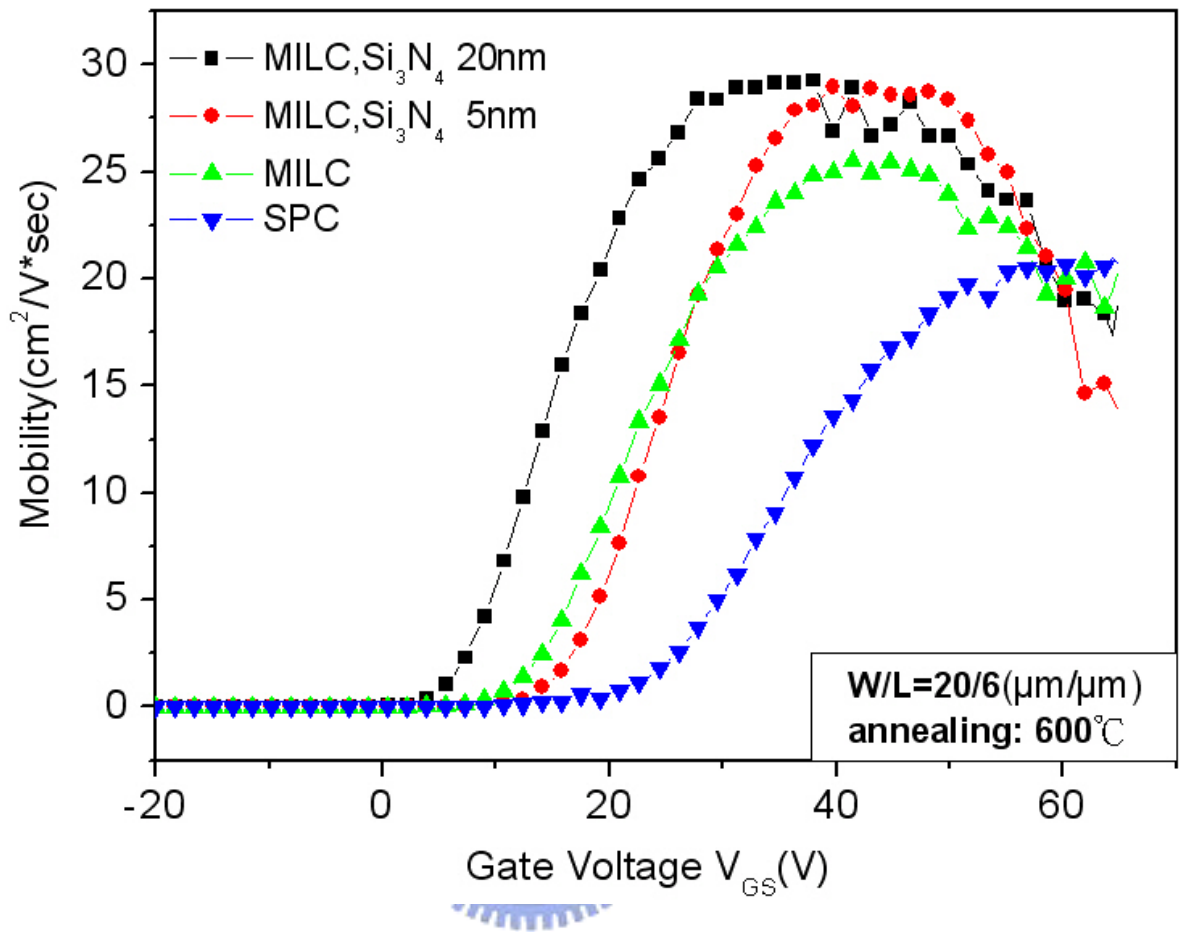


Figure 3.4 Comparison of mobility for MILC TFT's with and without  $\text{Si}_3\text{N}_4$  filter layer at  $V_{DS}=0.1\text{V}$ .

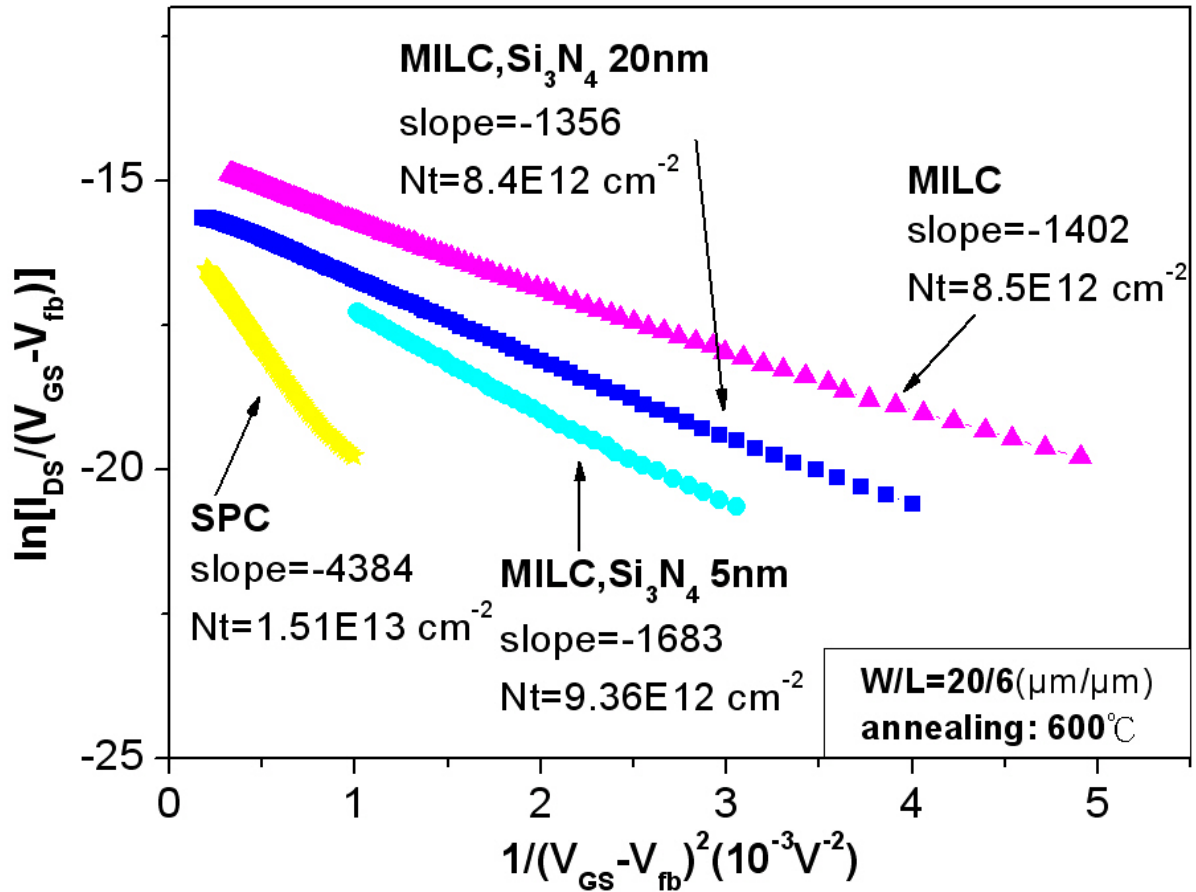


Figure 3.5 Extraction of  $Nt$  by modified Levinson theorem for comparison of MILC TFT's and SPC TFT's.



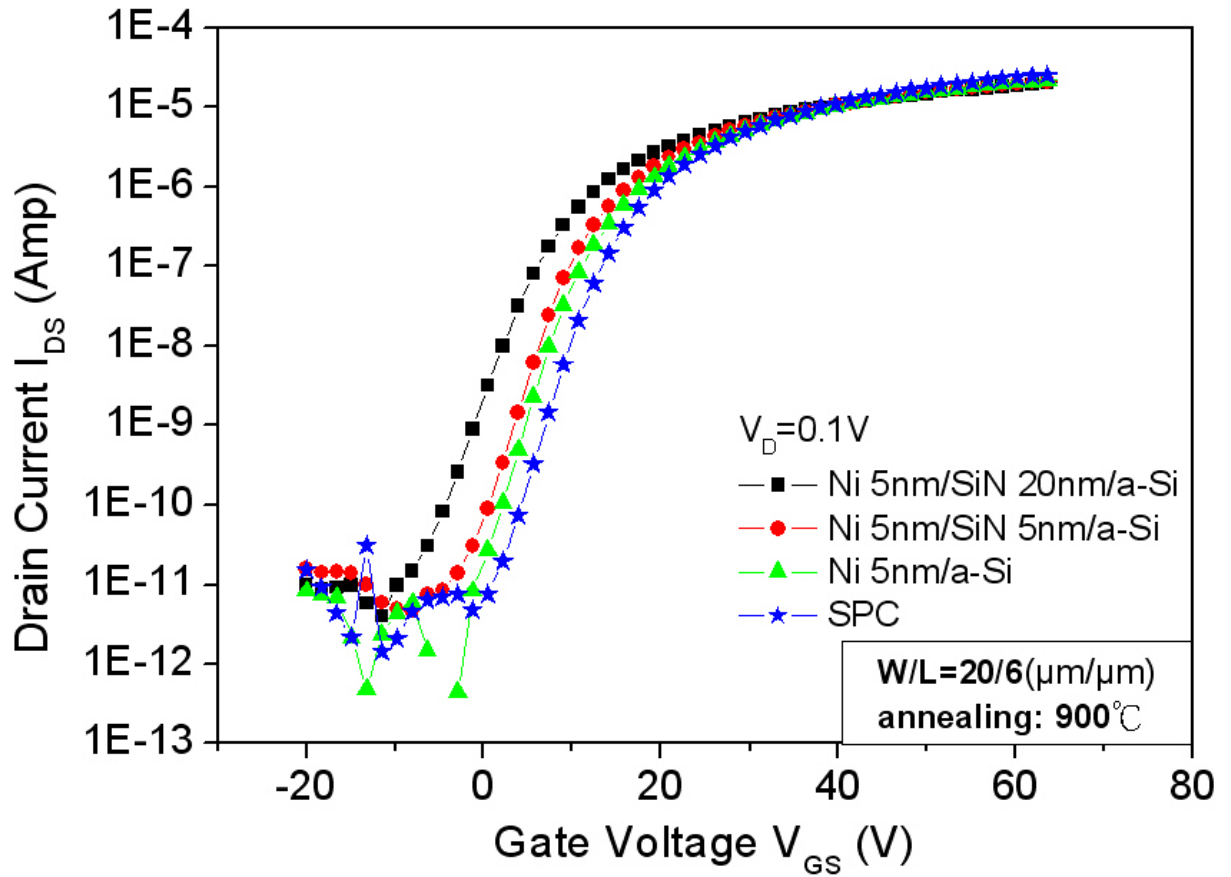


Figure 3.6 Transfer characteristics for comparison of MILC TFT's with and without  $\text{Si}_3\text{N}_4$  filter layer ( $V_D=0.1V$ ).

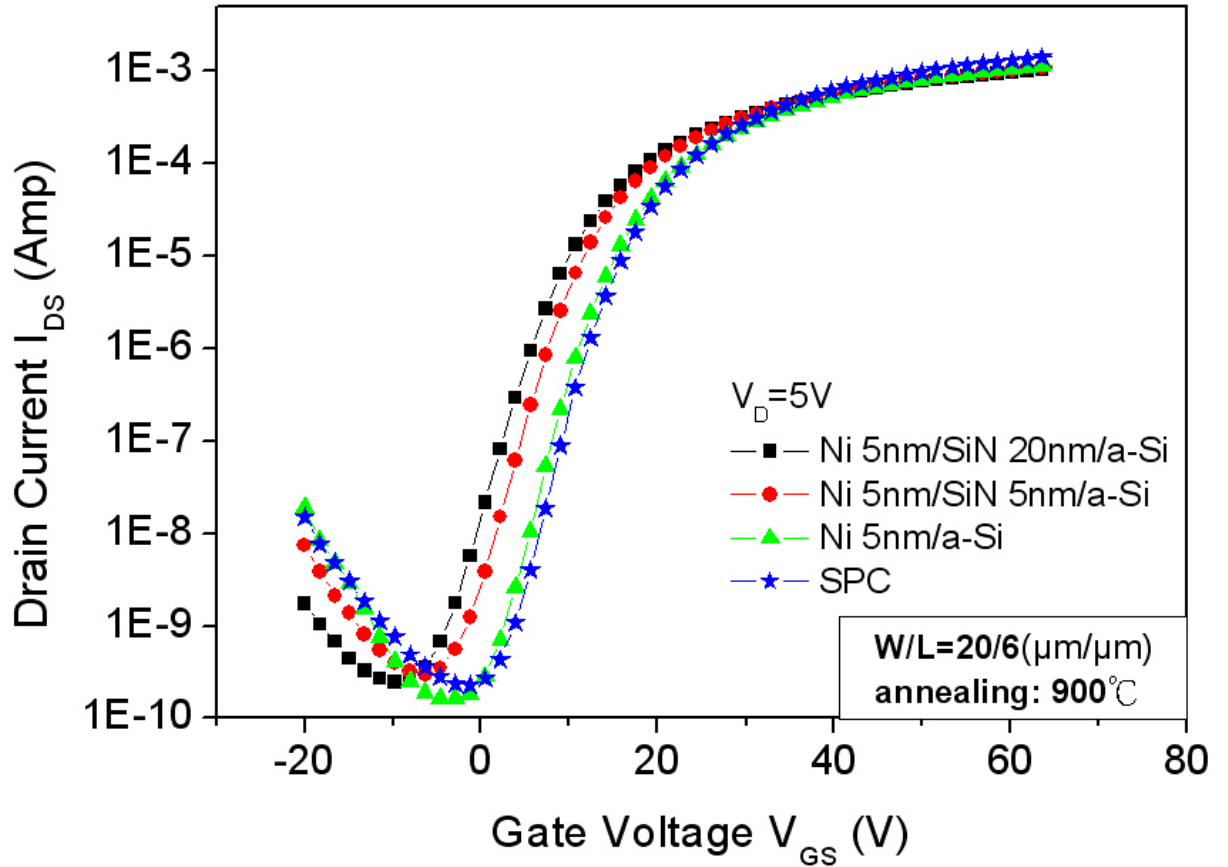


Figure 3.7 Transfer characteristics for comparison of MILC TFT's with and without  $\text{Si}_3\text{N}_4$  filter layer ( $V_D=5V$ ).

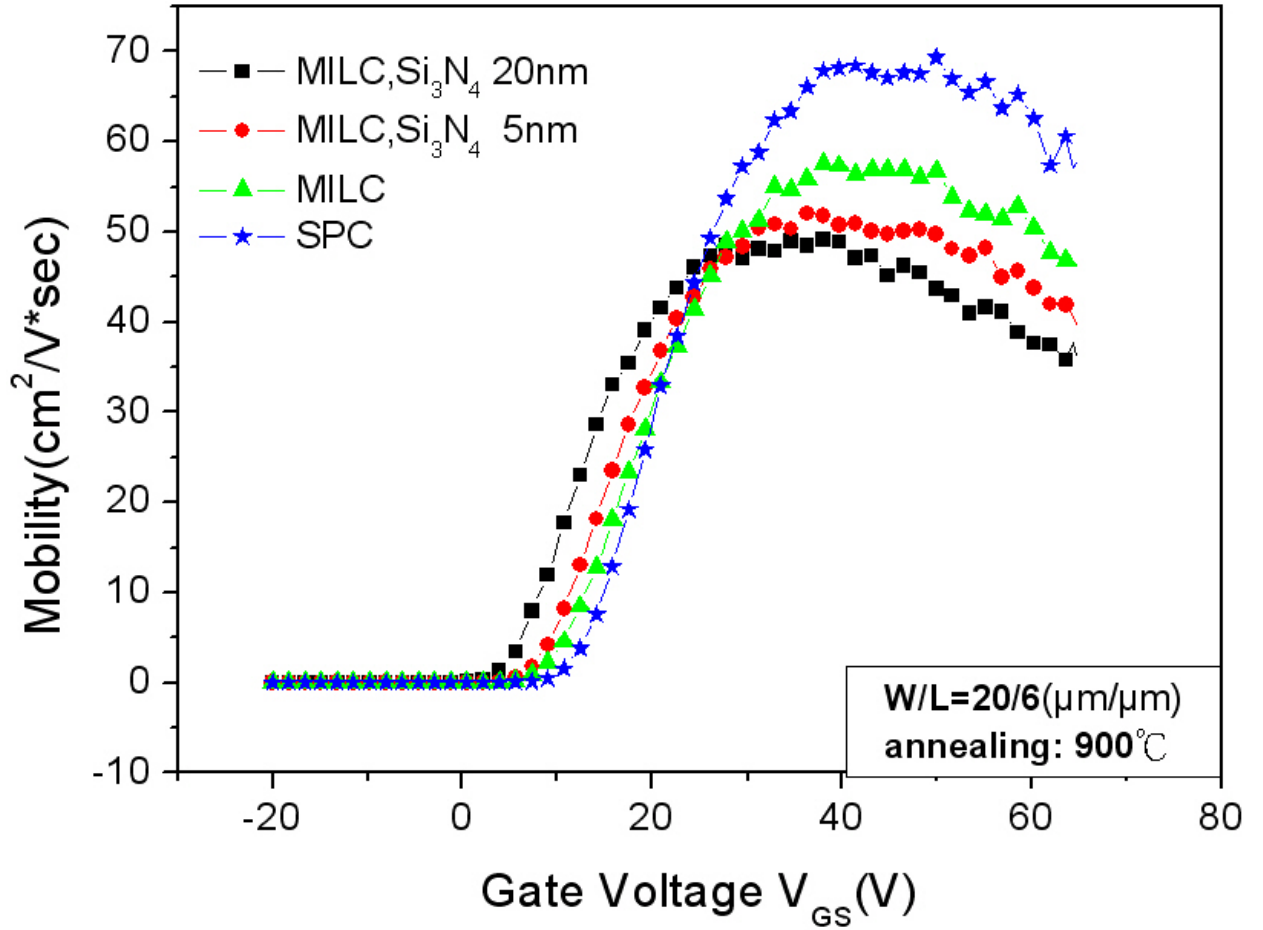


Figure 3.8 Comparison of mobility for MILC TFT's with and without Si<sub>3</sub>N<sub>4</sub> filter layer at V<sub>DS</sub>=0.1 V.

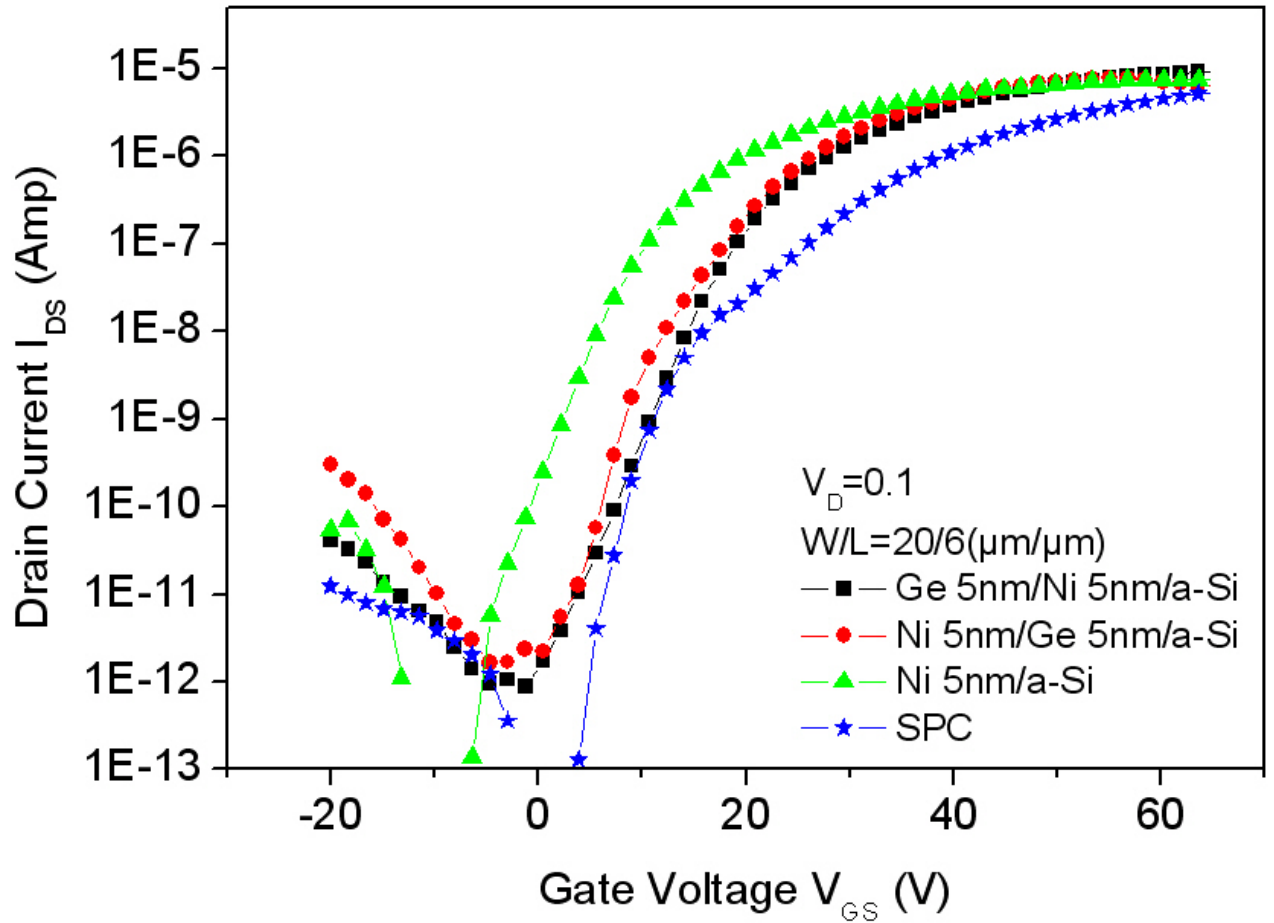


Figure 3.9 Transfer characteristics for MILC TFT's deposited Ge layer ( $V_D = 0.1$  V).

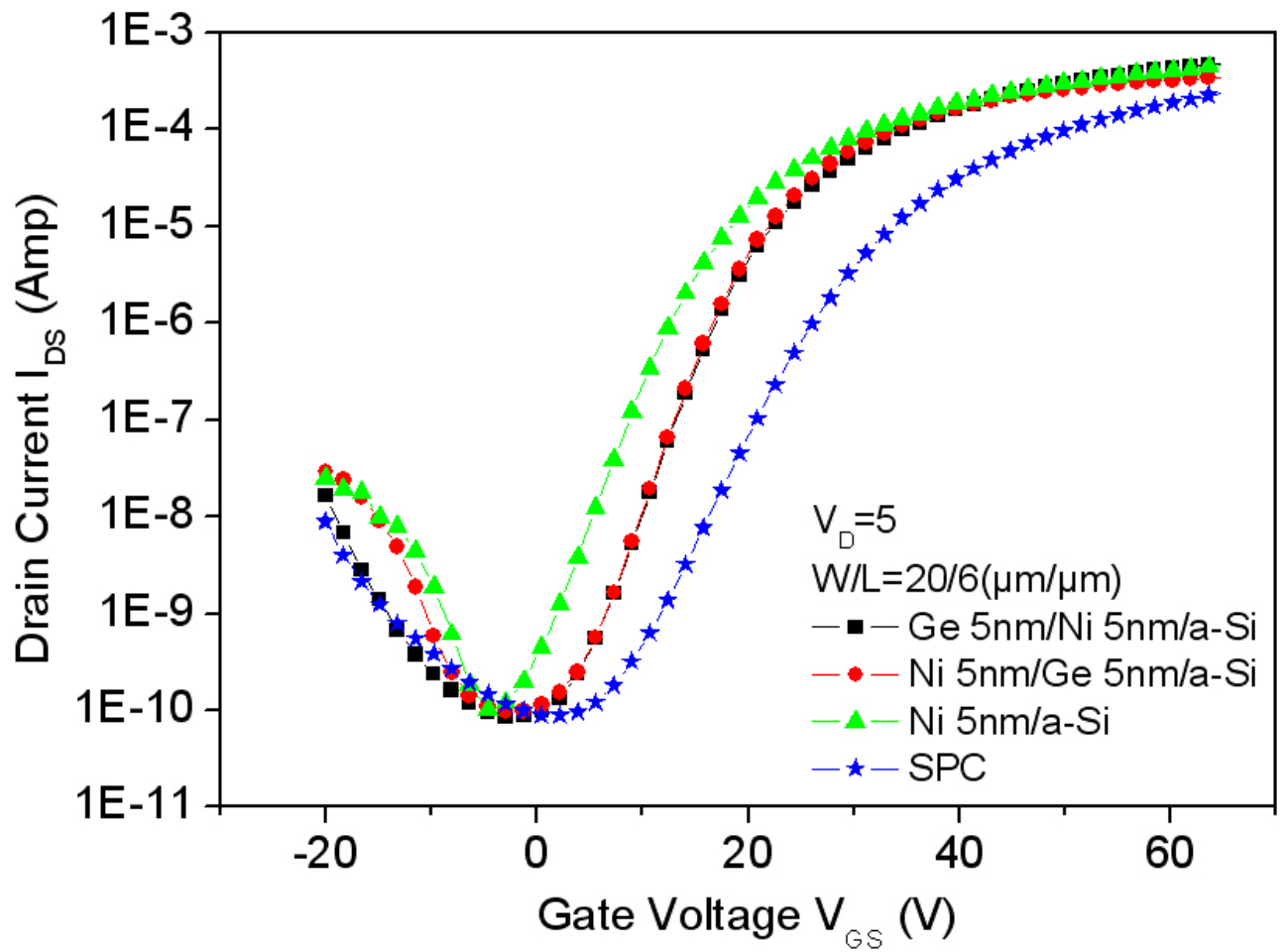


Figure 3.10 Transfer characteristics for MILC TFT's deposited Ge layer ( $V_D = 5\text{V}$ ).

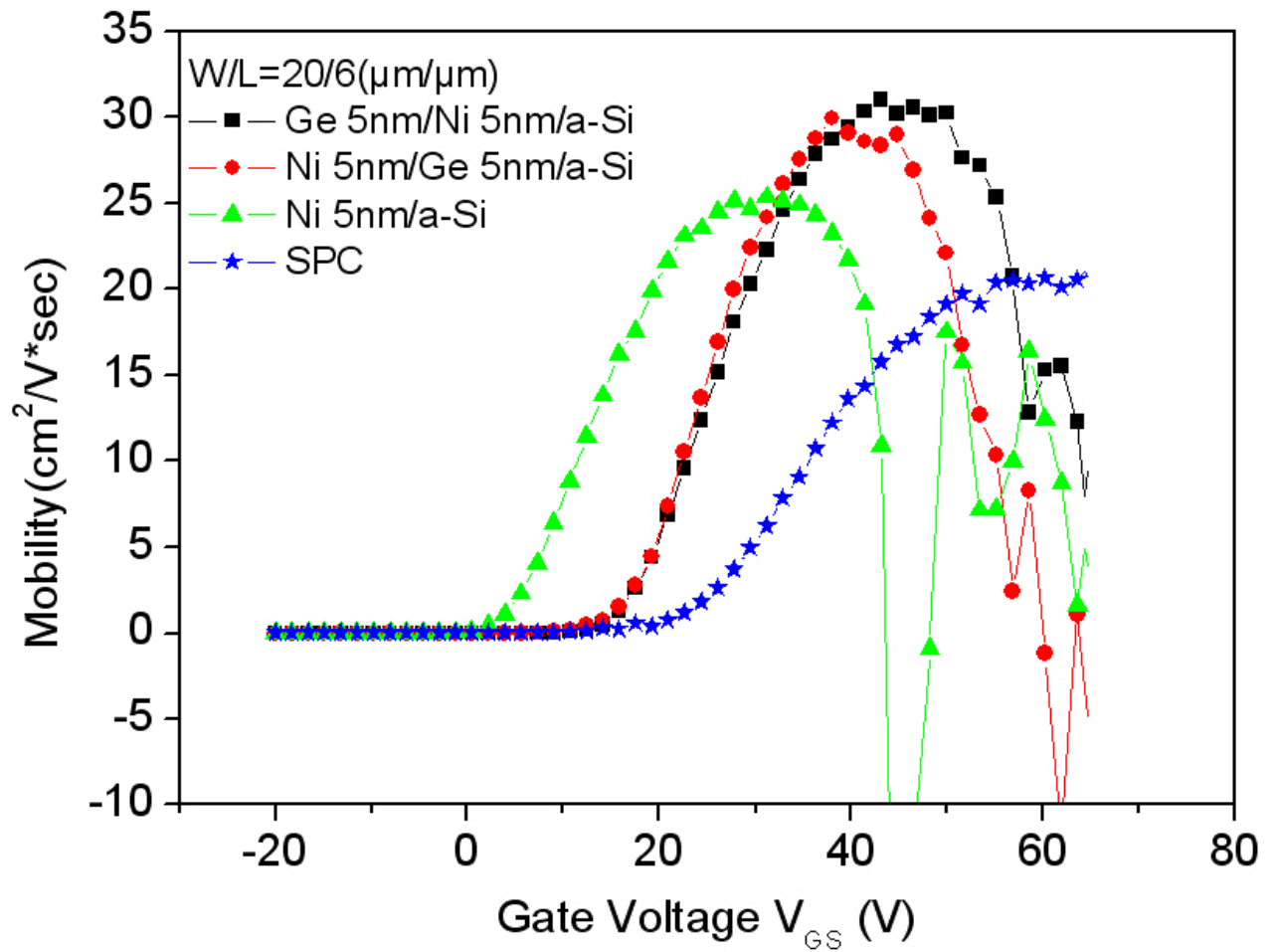


Figure 3.11 Comparison of mobility for MILC TFT's deposited Ge layer at  $V_{DS}=0.1\text{V}$ .

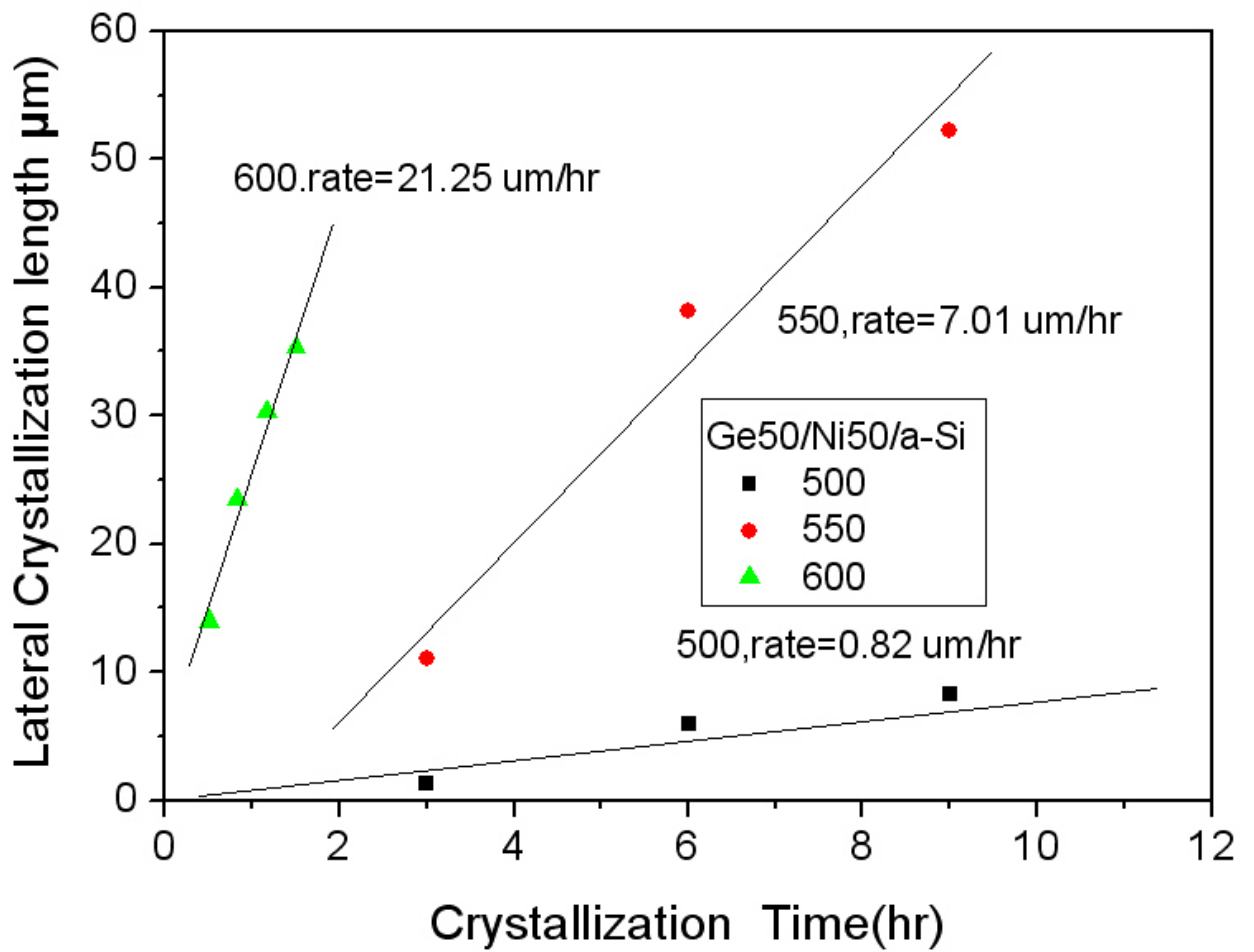


Fig. 3-12 Crystallization rate for Ge 5nm/ Ni 5nm/ a-Si deposited structure at different temperature.

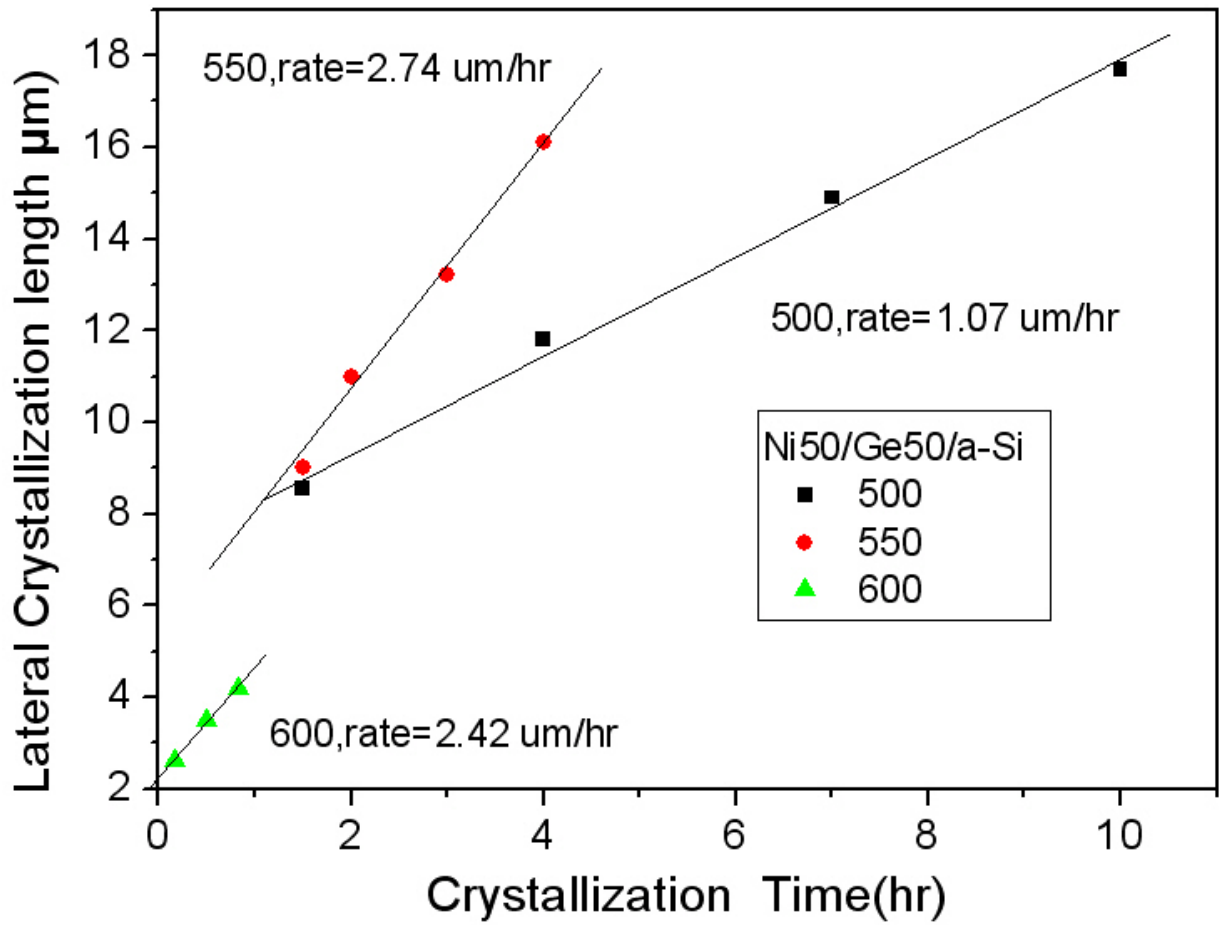


Fig. 3-13 Crystallization rate for Ni 5nm/ Ge 5nm/ a-Si deposited structure at different temperature.



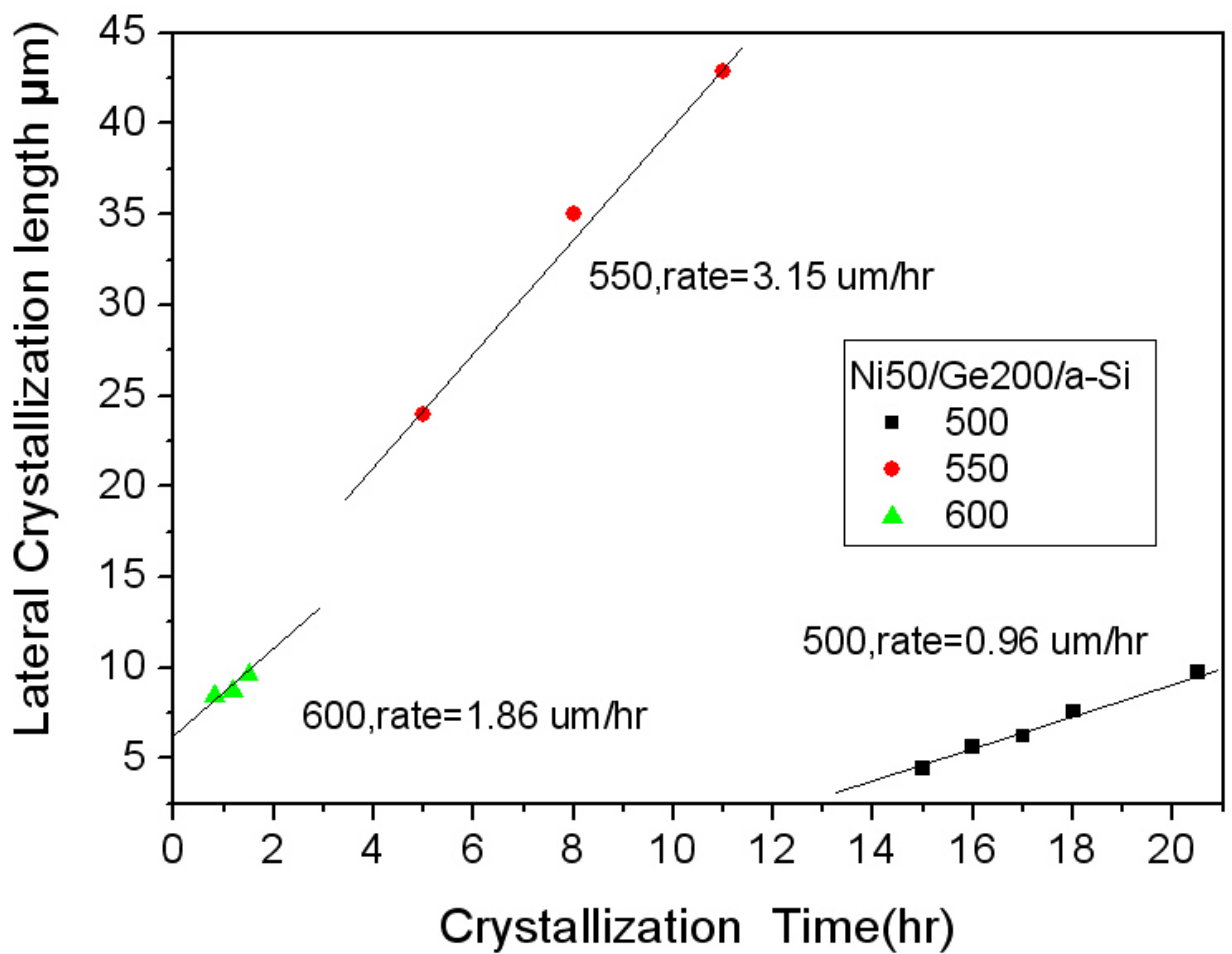


Fig. 3-14 Crystallization rate for Ni 5nm/ Ge 20nm/ a-Si deposited structure at different temperature.

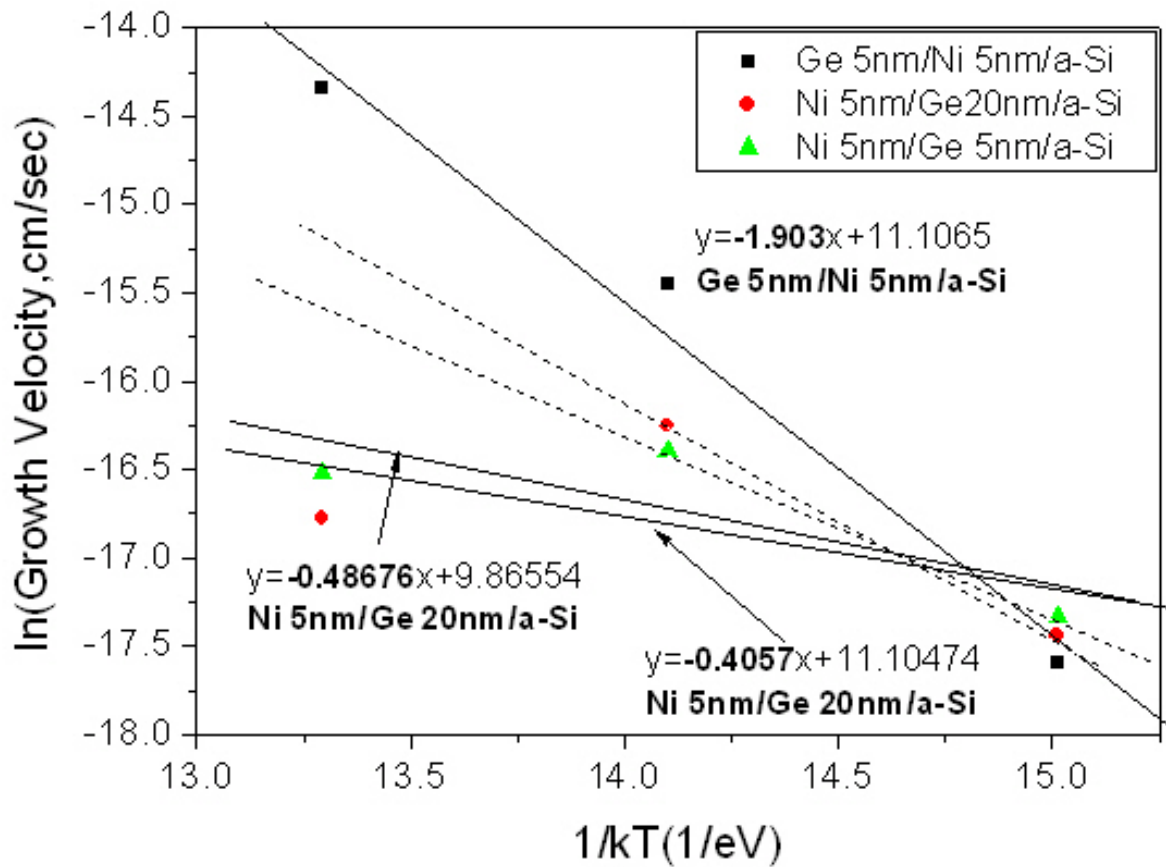


Fig. 3-15 Arrhenius plots and extracting of  $E_a$  and  $r_0$  for different samples.

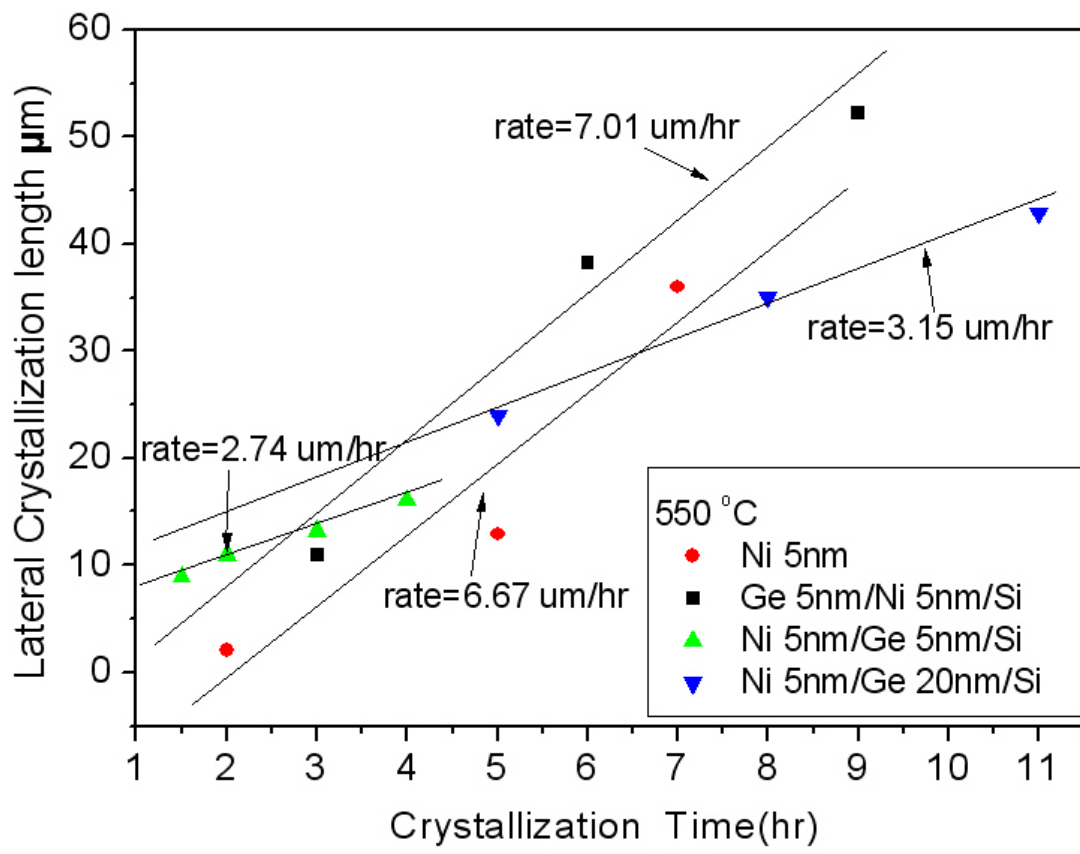
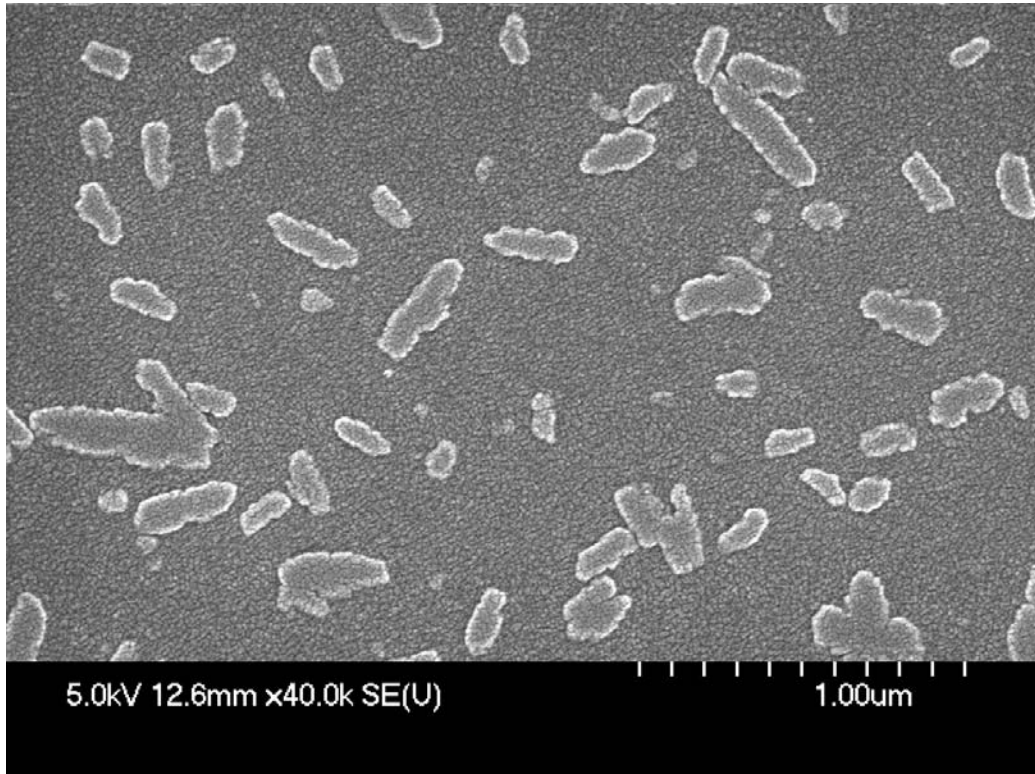
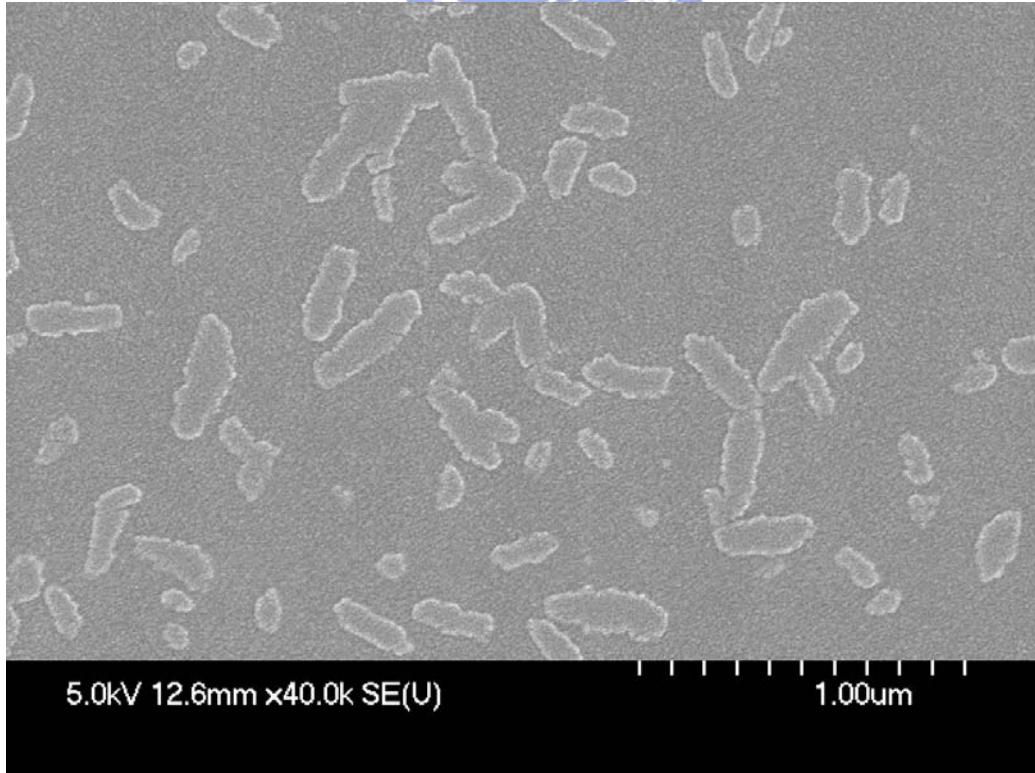


Fig. 3-16 Crystallization rate for different deposited metal structure at 550 °C.

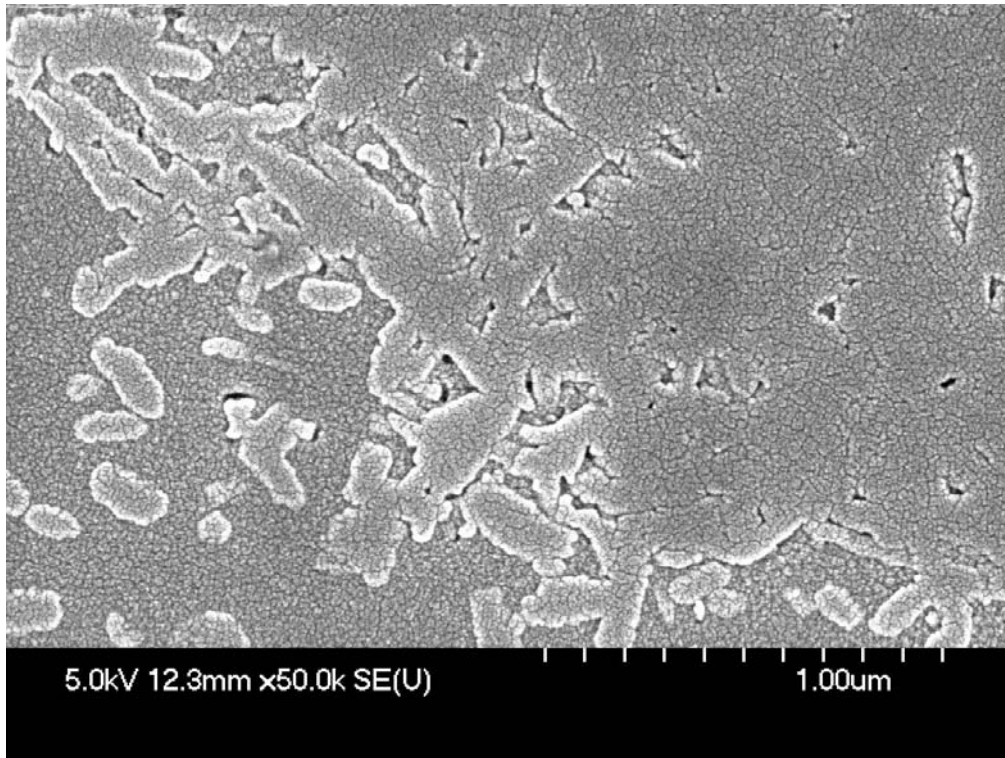


(a) Ni 5nm/Ge 5nm/a-Si

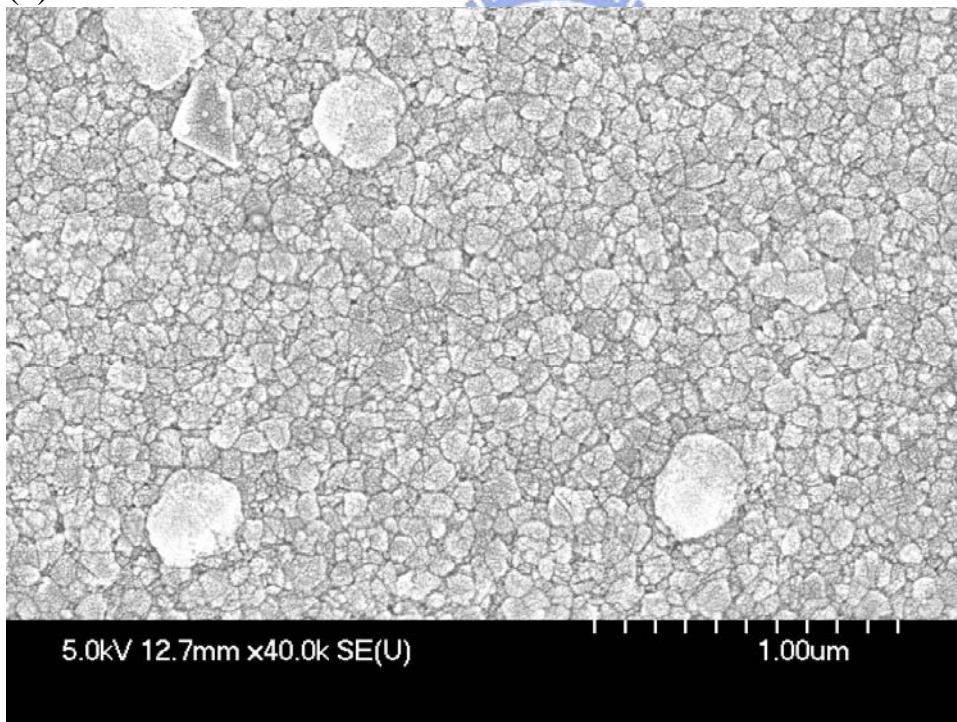


(b) Ni 5nm/Ge 20nm/a-Si





(c) Ge 5nm/Ni 5nm/a-Si



(d) Ni 5nm/Si<sub>0.85</sub>Ge<sub>0.15</sub>

Fig.3-17 SEM graph of Secco-etched Ni MILC Poly -Si for difference structure ,after 6 hr at 550 °C:

(a) Ni 5nm/Ge 5nm/a-Si, (b) Ni 5nm/Ge 20nm/a-Si, (c) Ge 5nm/Ni 5nm/a-Si, (d) Ni 5nm/Si<sub>0.85</sub>Ge<sub>0.15</sub>

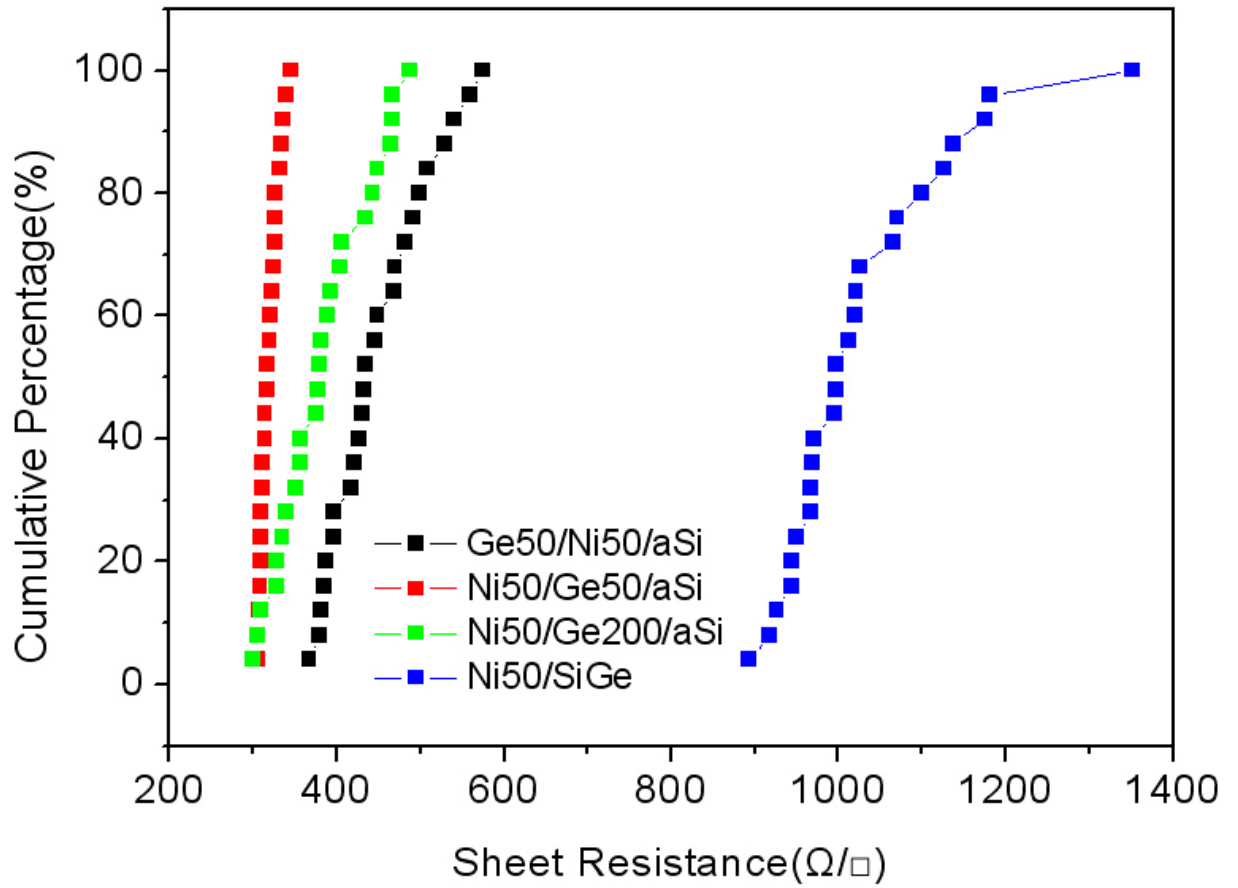


Fig.3-18 Sheet resistance for metal-induced crystallization after 24 hr at 550°C.